J Neurophysiol 93: 1809–1815, 2005.
First published October 13, 2004; doi:10.1152/jn.00629.2004.

Report

Contrast Dependence of Suppressive Influences in Cortical Area MT of Alert Macaque

Christopher C. Pack, J. Nicholas Hunter, and Richard T. Born
Department of Neurobiology, Harvard Medical School, Boston, Massachusetts

Submitted 21 June 2004; accepted in final form 8 October 2004

Pack, Christopher C., J. Nicholas Hunter, and Richard T. Born. Contrast dependence of suppressive influences in cortical area MT of alert macaque. *J Neurophysiol* 93: 1809–1815, 2005. First published October 13, 2004; doi:10.1152/jn.00629.2004. Visual neurons are often characterized in terms of their tuning for various stimulus properties, such as shape, color, and velocity. Generally, these tuning curves are further modulated by the overall intensity of the stimulus, such that increasing the contrast increases the firing rate, up to some maximum. In this paper, we describe the tuning of neurons in the middle temporal area (MT or V5) of macaque visual cortex for moving stimuli of varying contrast. We find that, for some MT neurons, tuning curves for stimulus direction, speed, and size are shaped in part by suppressive influences that are present at high stimulus contrast but weak or nonexistent at low contrast. For most neurons, the suppression is direction-specific and strongest for large, slow-moving stimuli. The surprising consequence of this phenomenon is that some MT neurons actually fire more vigorously to a large low-contrast stimulus than to one of high contrast. These results are consistent with recent perceptual observations, as well as with information-theoretic models, which hypothesize that the visual system seeks to reduce redundancy at high contrast while maintaining sensitivity at low contrast.

INTRODUCTION

Neurons in the middle temporal area (MT or V5) of the primate visual cortex are tuned for the direction of stimulus motion (Dubner and Zeki 1971). In addition to direction tuning, many MT neurons exhibit tuning for stimulus size (Allman et al. 1985) and speed (Maunsell and Van Essen 1983), suggesting that individual neurons may perform rather sophisticated calculations on the visual input (Buracas and Albright 1996; Gautama and Van Hulle 2001). Physiological studies have found that MT tuning for stimulus size is due to a mechanism that suppresses responses to stimuli that extend beyond a neuron's classical receptive field (Allman et al. 1985; Born 2000; Xiao et al. 1995). Similarly, suppressive influences have been found to be involved in shaping the selectivity of MT neurons for stimulus speed and direction (Mikami et al. 1986).

In the primary visual cortex (V1), contrast modulates suppressive influences on spatial (Anderson et al. 2001; Cavanaugh et al. 2002; Kapadia et al. 1999; Levitt and Lund 1997; Polat et al. 1998; Sceniak et al. 1999) and temporal (Albrecht 1995; Frazor et al. 2004) receptive field structure. To determine if similar effects are seen in MT, we used stimuli of differing contrast to characterize the influence of suppression on the tuning of MT neurons for stimulus size, speed, and direction. The results suggest that, at high contrasts, suppression works primarily to reduce the responses of MT neurons to large, slow-moving stimuli. Functionally, this mechanism may serve to reduce redundancy in the visual input during self-motion.

METHODS

Extracellular recordings

Recordings were obtained from single units in two alert monkeys, as described previously (Born et al. 2000). Each animal underwent a MRI scan to locate MT within the coordinates of a plastic grid inserted in the recording cylinder. The same grid, along with a guide tube, was used to guide insertion of the microelectrode. MT was identified based on depth, prevalence of direction-selective neurons, receptive field size, and visual topography. Neuronal signals were recorded extracellularly using tungsten microelectrodes (FHC) with standard amplification and filtering (BAK Electronics), while the monkeys fixated a small spot. Fixation was monitored with an eye coil (Robinson 1963) and required to be within 1° of the spot for the monkeys to obtain a liquid reward. Single units were isolated using a dual time and amplitude window discriminator (BAK). All procedures were approved by the Harvard Medical Area Standing Committee on Animals.

Visual stimuli

Visual stimuli were presented on a computer monitor subtending 40 by 30° at a viewing distance of 57 cm. The refresh rate was 60 Hz. The stimuli consisted of random dot fields presented on a dim background (0.025 cd/m^2) and were viewed binocularly at a distance of 57 cm. The dot fields were presented in square apertures, with no blurring along the edges. Dot luminance was 139.5 cd/m^2 in the high-contrast condition and 2.2 cd/m^2 in the low-contrast condition. Using the SD of the luminance as a contrast metric (Martinez-Trujillo and Treue 2002; Molden et al. 1990) thus leads to values of 9.8 cd/m^2 for the high-contrast pattern and 0.7 cd/m^2 for the low-contrast pattern. Each dot subtended ~0.1°, and the average dot density was 0.5 dots/deg^2. For each neuron, we first collected a direction-tuning curve at high contrast, adjusting the size and speed manually to obtain robust responses from the neuron. We then measured speed tuning, and used the best speed and direction to obtain area summation curves. For speed tuning curves, the size of the stimulus was chosen to approximate the size of the classical receptive field, obtained by hand-mapping. The optimal speed, determined from the speed-tuning data at high contrast, was used in the collection of the area summation curves. For some cells, we also measured speed- and area-tuning in the null direction, defined to be 180° away from the preferred direction. Each stimulus was presented 5–10 times in block-wise random order for 1 s.

Address for reprint requests and other correspondence: C. Pack, Harvard Medical School, Dept. of Neurobiology, 220 Longwood Ave., Boston, MA 02115 (E-mail: cpack@hms.harvard.edu).

The costs of publication of this article were defrayed in part by the payment of page charges. The article must therefore be hereby marked "*advertisement*" in accordance with 18 U.S.C. Section 1734 solely to indicate this fact.

Data analysis

Data for each experiment were averaged over the full 1,000-ms stimulus presentation. Preferred speed was defined as the peak of a log-Gaussian fit to the mean firing rates. Each of the size-tuning curves was fit with two statistical models (DeAngelis and Uka 2003). The first was an error function, which is the integral of a Gaussian

$$R(w) = R_0 + A_e erf(w/\alpha)$$

where w is the stimulus size, R_0 is the baseline response, A_e is the excitatory amplitude, α is the size of the excitatory receptive field, and *erf* is the error function. The second model, a difference of error functions, corresponds functionally to a Gaussian-shaped center and surround, which interact through subtraction

$$R(w) = R_0 + A_e erf(w/\alpha) - A_i erf(w/\beta)$$

with A_i and β corresponding to the amplitude and size of the inhibitory surround. All stimulus fits were optimized via a least-squares criterion using the Levenberg-Marquardt algorithm in Matlab (Mathworks, Natick, MA).

Neurons were considered significantly surround suppressed if the addition of the second Gaussian improved the fit significantly (sequential F-test, $P < 0.05$). For these neurons, the preferred stimulus size was taken to be the peak of the data fit. For the rest of the neurons, the preferred size was taken to be the stimulus size at which the single error function fit reached 90% of its value (1.16α). Firing rate comparisons (Fig. 2, *D* and *H*) were performed on square-root transformed firing rates. The square-root transform is necessary to stabilize the variance in neuronal firing rates, which tends to increase with the mean (Prince et al. 2002).

RESULTS

We recorded from a total of 154 MT neurons in two alert macaque monkeys. Size-tuning curves were collected for 110 neurons, and speed-tuning curves were collected for 114 neurons. An additional 40 neurons were tested in both the preferred and null directions. The stimuli were random dot fields moving in the preferred direction for each cell, either at high or low contrast. Because the Michelson contrast commonly used with gratings does not translate well to nonperiodic stimuli, we used the SD of luminance as a contrast metric (Martinez-Trujillo and Treue 2002; Molden et al. 1990). This led to contrast values of 9.8 cd/m^2 for the high-contrast pattern and 0.7 cd/m^2 for the low-contrast pattern.

Size tuning and contrast

Many neurons showed dramatically different tuning in the two contrast conditions, and one such example is shown in Fig. 1*A* (dashed line). At low contrast, the response of this neuron increased as the stimulus diameter increased, and this trend continued up to the largest stimulus tested, which was 35° in diameter. At high contrast (solid line), this neuron responded strongly to small stimuli moving in its preferred direction, with a peak response for a stimulus that was 10° in diameter. However, when the stimulus diameter was increased beyond 15°, the neuron's response was substantially lower than in the low-contrast condition, even though the direction, speed, and spatial position of the stimulus were the same in both conditions.

For the majority of the neurons tested in this manner (69/110), the most effective stimulus at low contrast was larger than the most effective stimulus at high contrast. The median difference in preferred stimulus size (see METHODS) between the high- and low-contrast conditions was 4.2°. This corresponded to an average increase of 28%.

Preference for a particular stimulus size is often related to the strength and spatial extent of a neuron's inhibitory surround. The surround suppresses the response to large stimuli, so that many neurons, such as the one in Fig. 1*A* (at high

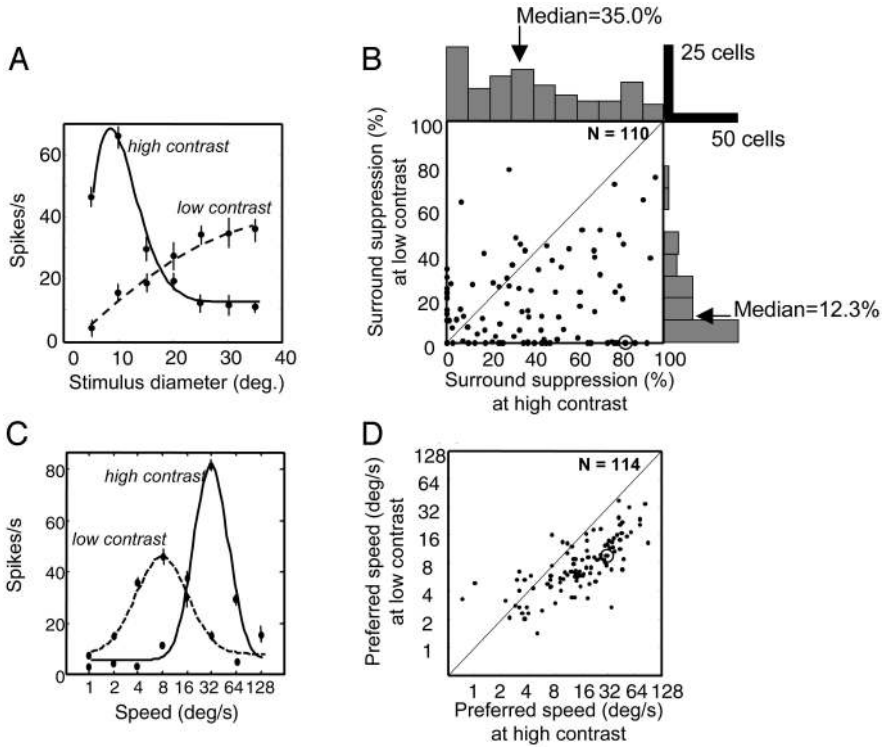

FIG. 1. Influence of contrast on middle temporal area (MT) tuning curves. *A*: size-tuning of a single MT neuron at low (dashed line) and high (solid line) contrasts. For the high-contrast data, the best-fitting difference of error functions is shown. For the low-contrast data, the best-fitting error function is shown. Error bars represent SE. *B*: change in suppression index between the low- and high-contrast conditions across the MT population ($n = 110$). Each dot represents a neuron, and the solid diagonal line indicates points where the suppression index was unchanged with contrast. Circled dot corresponds to the cell in *A*. *C*: speed-tuning of a single MT neuron at low (dashed line) and high (solid line) contrasts. For both speed-tuning curves, the best-fitting log-Gaussian function is shown. Error bars represent SE. *D*: change in preferred speed between the low- and high-contrast conditions across the MT population ($n = 114$) Circled dot corresponds to the cell in *C*.

contrast), respond best to relatively small stimuli. To quantify the amount of surround suppression under both contrast conditions, we used a *suppression index*, defined simply as the reduction in response between the largest (35°) stimulus and the stimulus that elicited the peak response. Thus the suppression index for the cell in Fig. 1*A* was 83% at high contrast and 0% at low contrast. As shown in Fig. 1*B*, the majority of neurons exhibited a response pattern that was qualitatively similar to that of the neuron shown in Fig. 1*A*. For the population of 110 cells, the median surround suppression in the high contrast condition was 35.0%, whereas in the low contrast condition, this figure fell to 12.3%. In fact, many neurons lost their surround suppression entirely when the contrast was low, as shown by the dots that fall along the *x*-axis of Fig. 1*B*.

Another way to measure surround suppression is to fit the data with a difference of error functions (DeAngelis and Uka 2003; Sceniak et al. 1999) (see METHODS). Each error function is the integral of a Gaussian, and the two Gaussians correspond to the excitatory center and inhibitory surround of the receptive field. For neurons with minimal surround suppression (Fig. 1*A*, low contrast), the size-tuning curve is determined entirely by the excitatory receptive field, so a single error function is sufficient to model the data. However, a single error function cannot model surround suppression, so for many neurons, a second, inhibitory, error function is required. This influence can be quantified by measuring the extent to which the inhibitory function improves the data fit (DeAngelis and Uka 2003). Overall, the size-tuning curves were well fit by this approach, with a median R^2 of 0.95. For 40/110 neurons (36%), the inclusion of the second error function improved the fit with the high-contrast data significantly (sequential *F*-test, $P < 0.05$). In the low-contrast condition, this figure fell to 9% (10/110). For the 40 cells with significant surround suppression at high contrast, the sizes of the excitatory and inhibitory Gaussians were highly correlated (linear regression, $P < 0.05$, $r^2 = 0.64$). The ratio of surround sizes to center sizes had a geometric mean of 1.7.

Speed tuning and contrast

We observed a similar dependence of MT speed-tuning curves on contrast. Figure 1*C* shows the responses of an example neuron to moving stimuli of optimal direction, spatial position, and size. In the low-contrast condition (dashed line), the neuron was broadly tuned to speed, with a peak response to motion at 8°/s. When the contrast was increased (solid line), the tuning curve shifted, so that the neuron was almost completely silent for speeds below 8°/s and responded best to a speed of 32°/s.

To quantify the effect of contrast on speed tuning, we fit each speed-tuning curve with a log-Gaussian function. All of the speed-tuning curves were well fit by this function, with R^2 values ranging from 0.85 to 0.99 (median, 0.96). Taking the preferred speed for each neuron to be the peak of the log-Gaussian fit, we found that a contrast-dependent shift in speed preference occurred for nearly every MT neuron we tested. Such shifts were particularly prominent for neurons tuned to high speeds at high contrast, as shown in Fig. 1*D*. Across the population of 114 neurons, the median preferred speed was 14.5°/s (SD; 1.4 octaves) in the high-contrast condition and 6.7°/s (1.08 octaves) in the low-contrast condition. These values are on the low end of published reports of average preferred speed, which range from around 6 (Lagae et al. 1993) to 40°/s (Rodman and Albright 1987), depending on the spatial composition on the stimulus (Priebe et al. 2003). The mean difference in preferred speed between the low- and high-contrast conditions was 1.2 ± 0.9 octaves.

In addition to changes in preferred speed, many neurons exhibited a change in the width of tuning with changes in contrast. The neuron in Fig. 1*C* is an example of a cell that was narrowly tuned at high contrast and broadly tuned at low contrast. This was generally the case with neurons tuned to high speeds at high contrast. Conversely, cells tuned to low speeds at high contrasts exhibited an increase in tuning width with increasing contrast. Across the population, preferred speed at high contrast was negatively correlated with contrast-dependent changes in bandwidth (linear regression, $P < 0.00002$). On average, neurons with preferred speeds <14.5°/s ($n = 57$) showed an increase in bandwidth of 51%, whereas those with preferred speeds >14.5°/s ($n = 57$) showed a decrease in bandwidth of 38%. Thus increasing the contrast increased the bandwidth for slow-tuned neurons and decreased the bandwidth for fast-tuned neurons.

Firing rate and contrast

The preceding analysis described the effect of stimulus contrast on MT tuning curves, irrespective of absolute firing rate. We next examined the differences in firing rates in response to high- and low-contrast stimuli of differing size and speed. In the example shown in Fig. 1*A*, the shift in size-tuning was due to a firing rate increase (facilitation) for small stimuli (<20°) and a firing rate decrease (suppression) for large stimuli (>20°). This point is further shown in Fig. 2*A*, which shows the result of subtracting the low-contrast response from the high-contrast response for the same neuron. Facilitation is indicated by points above the dotted line, and suppression corresponds to points below the dotted line. Figure 2*C* shows the same analysis for a neuron that lacked surround suppression. In this case, the difference tuning curve shows no suppression at any stimulus size and a large facilitation for the largest stimulus size.

To summarize these effects across the MT population, we constructed difference curves like the ones in Fig. 2, *A–C*, for each of 110 MT neurons. Each tuning curve was normalized to the neuron's maximum firing rate across all stimulus conditions and ranked according to the suppression index obtained in the high-contrast condition. The results for the population are displayed in Fig. 2*D*. Here, each horizontal row corresponds to the difference curve for one neuron, with orange corresponding to facilitation and blue to suppression. The neurons are shown in increasing order of suppression index from bottom to top, so that the lower rows correspond to neurons, like the one shown in Fig. 2*C*, that had no surround suppression. Neurons that were strongly surround-suppressed, like the one in Fig. 2*A*, are shown in the *top rows* of Fig. 2*D*. Thus the blue region in the *top right* of Fig. 2*D* indicates that neurons with strong surround suppression responded better to large stimuli at low contrast than at high contrast. For the largest stimulus size tested, this change in firing rate was significant in 24 neurons (22%) ($P < 0.05$, *t*-test on square-root transformed firing rates). The average high-contrast suppression index for this group of cells was

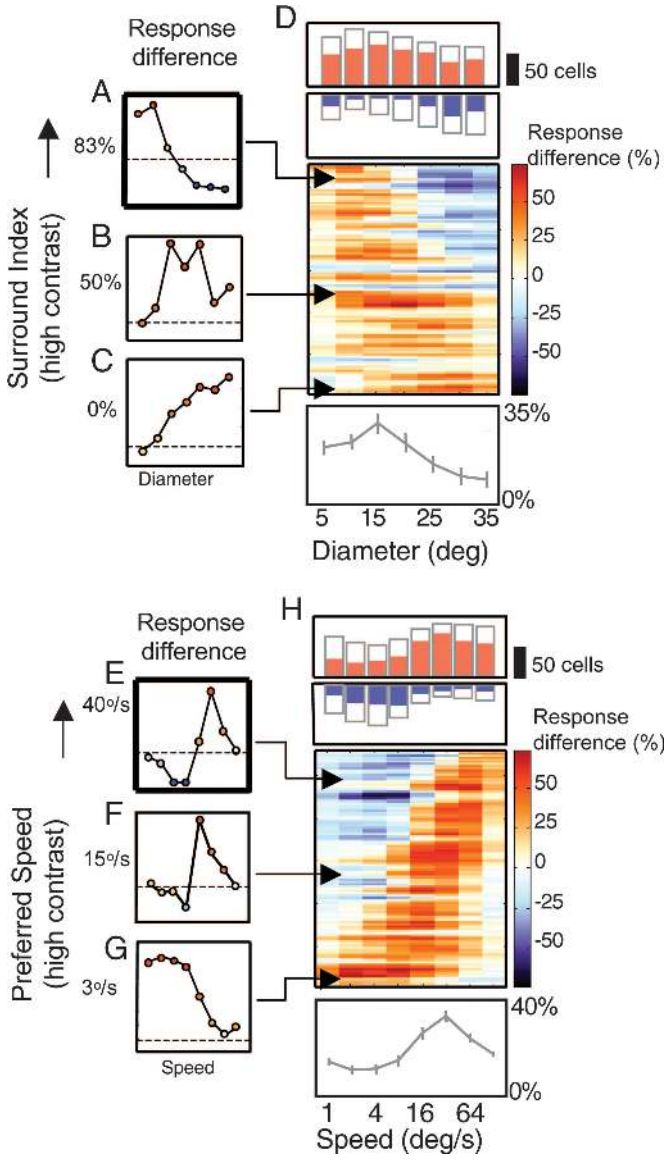

FIG. 2. Difference between high- and low-contrast responses in MT. *A–C*: results of subtracting low-contrast size-tuning curve from high-contrast size-tuning curve for neurons with differing amounts of surround suppression. *D*: difference tuning curves for every neuron in the population ($n = 110$). Blue regions indicate suppression, and orange regions indicate facilitation. Map was smoothed with a Gaussian (3 pixel SD) to highlight the trends in population data. Histograms above the plot show incidence of facilitatory and suppressive responses as a function of stimulus size. *Top histogram*: number of cells showing positive differences. *Bottom histogram*: number of cells showing negative differences. Solid bars indicate number of cells with response differences that were statistically significant. Below the population map is shown the average difference for all cells recorded. Error bars shown SE. *E–G*: results of subtracting low-contrast speed-tuning curve from high-contrast speed-tuning curve for neurons with different preferred speeds. *H*: difference tuning curves for every neuron in the population ($n = 114$) as in *D*.

50 ± 23% compared with 23 ± 20% for neurons that showed a significant increase in firing at the largest stimulus size. Thus neurons with strong surround suppression decrease their responses to large stimuli as contrast is increased.

The histograms at the *top* of Fig. 2*D* show the prevalence of facilitatory and suppressive effects at different stimulus sizes. Solid bars indicate effects that were statistically significant at the $P = 0.05$ level, according to a one-tailed *t*-test on square-root transformed firing rates. Overall, suppression was most common for large stimulus sizes, whereas facilitation occurred primarily for smaller stimuli.

One possible explanation for this finding is that the neurons were simply unresponsive at low contrasts and suppressed below baseline at high contrasts. Suppression below baseline has previously been reported for null-direction stimulation (Mikami et al. 1986). However, this does not explain our results, because in the high-contrast condition, suppression below baseline was observed for just 3/110 neurons at nonpreferred sizes and 8/114 at nonpreferred speeds.

Tuning curves for speed showed a similar, differential effect of contrast. Figure 2*E* shows the difference between the high- and low-contrast speed-tuning curves for the neuron shown in Fig. 1*C*. When contrast was increased, this neuron's response was suppressed at low speeds and facilitated at high speeds. A second neuron, which preferred low speeds, showed facilitation for slow stimuli, but its response was unchanged for fast stimuli (Fig. 2*G*). Figure 2*H* shows the relative magnitudes of facilitation and suppression for the population of 114 neurons. In this figure, the tuning curves are arranged in ascending order of preferred speed in the high contrast condition from *bottom* to *top*. Here the blue regions in the *top left* of the figure indicate high-contrast suppression for low stimulus speeds, and the histograms indicate the prevalence of these findings across the population.

The data in Fig. 2 show that tuning for speed and size changes with stimulus contrast. For many neurons, the change is due primarily to suppressive influences that are specific to particular types of stimuli. This raises the possibility that the suppression found in the speed- and area-tuning curves share a common mechanism. For the 70 cells for which we had both speed- and size-tuning data at different contrasts, we compared the contrast-dependent shift in preferred speed with the contrast-dependent change in surround suppression. These measures were indeed correlated (linear regression, $P < 0.01$, $r^2 = 0.10$). For the high-contrast data, there was also a correlation between preferred speed and the suppression index (linear regression, $P < 0.001$, $r^2 = 0.22$), indicating that cells tuned to high speeds were more strongly surround suppressed. Both of these correlations were statistically significant, but rather weak, suggesting that multiple mechanisms may contribute to the observed suppression. For instance, our stimuli did not probe the heterogeneity of surround structure, which in many neurons is dependent on stimulus speed (Xiao et al. 1995).

Direction tuning and contrast

For 40 neurons, we repeated the contrast comparison for stimuli moving in the null direction. This revealed a third type of high-contrast suppression: most MT neurons responded more strongly to motion in the null direction at low contrasts than at high contrasts. This sharpening of direction selectivity was evident in most neurons across the entire range of stimulus speeds and sizes tested. Figure 3, *A–D*, show size- and speed-tuning curves for one example MT cell. The solid lines indicate responses to preferred direction stimuli, and the dashed lines show those to null direction stimuli. In the size-tuning curves of Fig. 3, *A* and *B*, it is clear that the null direction stimuli elicit smaller responses in the high-contrast condition than in the

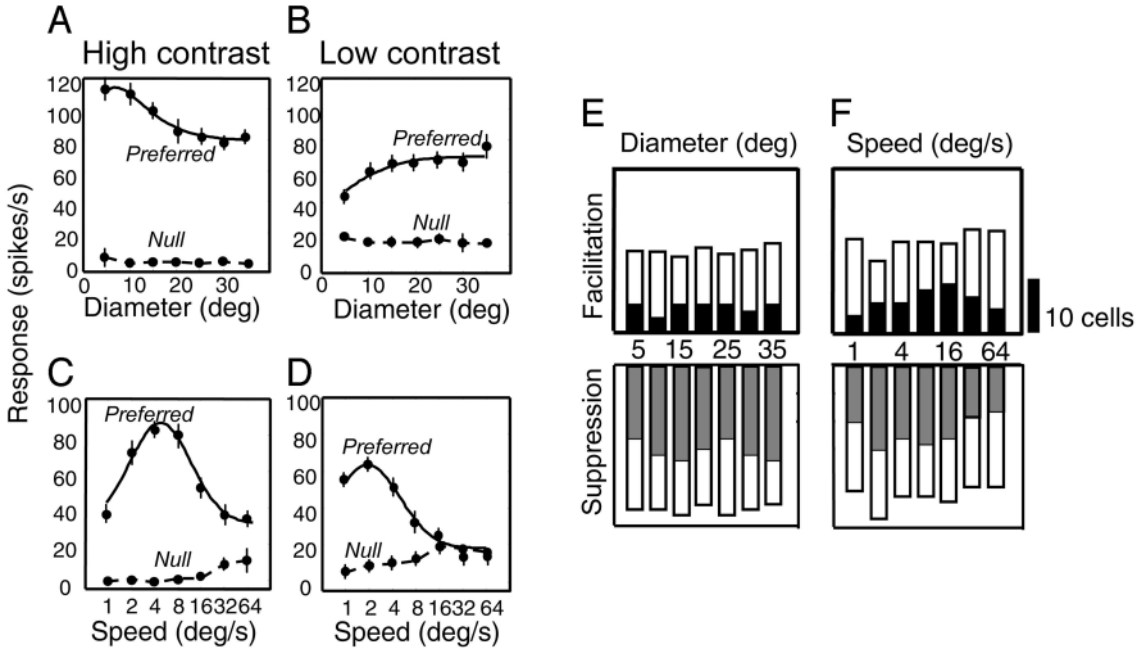

FIG. 3. Difference between high- and low-contrast responses to null-direction motion. *A*: response of a single MT neuron to high-contrast stimuli of varying sizes in the preferred (solid line) and null (dashed line) directions. For the preferred-direction data, the best-fitting difference of error functions is shown. *B*: as in *A*, but for low-contrast stimuli. For the preferred-direction data, the best-fitting error function is shown. *C*: response of a single MT neuron to high-contrast stimuli of varying speeds in the preferred (solid line) and null (dashed line) directions. For the preferred-direction speed-tuning curve, the best-fitting log-Gaussian function is shown. *D*: as in *C*, but for low-contrast stimuli. *E*: response differences across the MT population ($n = 40$) as a function of stimulus size for null-direction stimuli. These were obtained by subtracting low-contrast tuning curves from high-contrast tuning curves. Facilitation corresponds to the number of cells showing positive differences; suppression corresponds to the number of cells showing negative differences. *F*: as in *E*, but for speed-tuning curves. Solid bars indicate the number of cells showing statistically significant differences.

low-contrast condition. Similar results are seen in Fig. 3, *C* and *D,* for speed-tuning.

As in the preferred-direction experiments, we measured the effects of contrast by subtracting the low-contrast tuning curves from the high-contrast tuning curves. Unlike in the preferred-direction cases (Fig. 2), there was no general tendency for the suppression to favor particular speeds or sizes, so these data are not shown for the population. The relative frequencies of facilitation and suppression are summarized in the histograms of Fig. 3, *E* and *F*, which are analogous to those in Fig. 2, *D* and *H*. For null-direction stimulation, high-contrast suppression was more common than facilitation at all stimulus speeds and sizes.

As in the experiments with size- and speed-tuning, this result was not simply a consequence of the high-contrast stimulus suppressing null-direction responses below baseline. Although such suppression was observed for 19/40 cells in the high-contrast conditions, 16 of those 19 cells also showed null-direction suppression in the low-contrast condition. Thus our results indicate that the null-direction suppression previously described in MT (e.g., Mikami et al. 1986) is regulated by stimulus contrast.

DISCUSSION

We studied the influence of contrast on MT tuning curves for stimulus size, speed, and direction. In many neurons, these tuning curves appear to be influenced by one or more mechanisms that suppress neural responses at high contrast. These mechanisms primarily serve to reduce responses to large, slow-moving stimuli, as well as those to null-direction motion.

Contrast-dependent changes in the spatial and temporal properties of receptive fields have been reported previously for neurons in the retina (Barlow et al. 1957; Shapley and Victor 1978), lateral geniculate nucleus (Sclar 1987; Solomon et al. 2002), and primary visual cortex (Anderson et al. 2001; Cavanaugh et al. 2002; Frazor et al. 2004; Kapadia et al. 1999; Levitt and Lund 1997; Polat et al. 1998; Sceniak et al. 1999). Thus some of the effects we have found in MT are probably inherited from previous stages of visual processing. However, surround suppression for random dot stimuli is rare in the input layers of MT (Lagae et al. 1989), suggesting that some of the suppression is due to interactions within MT or feedback from other areas. In fact, surround suppression in V1 appears to be dependent in part on feedback from MT (Hupe et al. 1998), suggesting a more complex picture of suppressive influences in the cortex. Furthermore, the spatial scale of the suppressive influences in MT is considerably coarser than those attributable to feedforward inputs and intrinsic connections of V1 (Angelucci et al. 2002). Our data do not speak directly to these issues, which will have to be resolved through further experiments.

Our results on the contrast-dependence of surround suppression have recently been found to have a striking perceptual correlate in human observers. Tadin et al. (2003) reported that at high contrasts, the direction of large moving stimuli is harder to discriminate than that of small stimuli. Consistent with our findings on MT neurons, the situation reverses at low contrasts, so that large stimuli are more readily discriminated. However, while the perceptual effect is quite robust, our data suggest that only the most surround-suppressed MT cells show a decrease in response with increasing contrast. Furthermore, we have not

characterized the responses of MT neurons to stimuli that are not centered on the receptive field, as would be necessary to examine fully the relationship between neural and perceptual results.

Our data on speed tuning are a bit harder to reconcile with perceptual observations, which suggest that stimuli seem to move more slowly as contrast is decreased (Stone and Thompson 1992). We find that cells tuned to high speeds are strongly activated by slow stimuli at low contrasts (Fig. 1*D*), which would predict that observers should *overestimate* stimulus speed at low contrasts. It may be possible to resolve this discrepancy by assuming that the visual system is biased toward slow speeds when the total MT population activity is low (Priebe and Lisberger 2004; Weiss et al. 2002). Similarly, our results on surround suppression are consistent with the notion that inhibitory surrounds are relatively low in contrast sensitivity, biasing the system toward spatial integration at low contrast (Cavanaugh et al. 2002).

What purpose might such changes in receptive field structure serve? One possibility is that they are part of a strategy for maximizing information transmission through the visual pathways. Retinal motion is often caused by motion of the observer, in a way that depends on the type of animal and the structure of the environment. Nonetheless, the pattern of velocities on the retina during self-motion is quite consistent, following a $1/v^2$ distribution across a range of self-motion speeds and trajectories (van Hateren 1992a). Thus moving observers experience a preponderance of slow speeds, with directions that change very gradually across visual space. Consequently, the suppression observed in MT for large, slow stimuli can be thought of as a reduction in the redundancy in the input, a strategy that is familiar from information-theoretic approaches to visual processing (Attneave 1954; Shannon 1948).

Reducing redundancy is a useful strategy, provided that the input is high in contrast (Barlow 1961). However, at low contrast, the sole basis for distinguishing visual signal from random noise is the signal's regularity across space and time. In this case, preserving redundancy becomes critical, and spatial pooling and temporal summation are desired. Both of these theoretical results are consistent with our findings, and so they may provide a general framework for interpreting results on receptive field dynamics.

ACKNOWLEDGMENTS

P. Hendrickson provided excellent technical assistance, and D. Freeman developed some of the computer programs. We are especially grateful to Dr. Margaret Livingstone for the use of software and equipment.

GRANTS

This work was supported by National Science Foundation Cognitive Neuroscience Grant BCS-0235398 to C. C. Pack and National Eye Institute Grants EY-11379 and EY-12196 and the Kirsch Foundation to R. T. Born and EY-13135 (M. S. Livingstone).

REFERENCES

Albrecht DG. Visual cortex neurons in monkey and cat: effect of contrast on the spatial and temporal phase transfer functions. *Vis Neurosci* 12: 1191–1210, 1995.

Allman J, Miezin F, and McGuinness E. Direction- and velocity-specific responses from beyond the classical receptive field in the middle temporal visual area (MT). *Perception* 14: 105–126, 1985.

Anderson JS, Lampl I, Gillespie DC, and Ferster D. Membrane potential and conductance changes underlying length tuning of cells in cat primary visual cortex. *J Neurosci* 21: 2104–2112, 2001.

Angelucci A, Levitt JB, and Lund JS. Anatomical origins of the classical receptive field and modulatory surround field of single neurons in macaque visual cortical area V1. *Prog Brain Res* 136: 373–388, 2002.

Atick JJ and Redlich AN. What does the retina know about natural scenes? *Neural Comput* 4: 196–210, 1992.

Attneave F. Some informational aspects of visual perception. *Psychol Rev* 61: 183–193, 1954.

Barlow H. Possible principles underlying the transformation of sensory messages. In: *Sensory Communication*, edited by Rosenbluth WA. Cambridge, MA: MIT Press 1961, p. 217–234.

Barlow HB, Fitzhugh R, and Kuffler SW. Change of organization in the receptive fields of the cat's retina during dark adaptation. *J Physiol* 137: 338–354, 1957.

Born RT. Center-surround interactions in the middle temporal visual area of the owl monkey. *J Neurophysiol* 84: 2658–2669, 2000.

Born RT, Groh JM, Zhao R, and Lukasewycz SJ. Segregation of object and background motion in visual area MT: effects of microstimulation on eye movements. *Neuron* 26: 725–734, 2000.

Buracas GT and Albright TD. Contribution of area MT to perception of three-dimensional shape: a computational study. *Vision Res* 36: 869–887, 1996.

Cavanaugh JR, Bair W, and Movshon JA. Nature and interaction of signals from the receptive field center and surround in macaque V1 neurons. *J Neurophysiol* 88: 2530–2546, 2002.

DeAngelis GC, and Uka T. Coding of horizontal disparity and velocity by MT neurons in the alert macaque. *J Neurophysiol* 89: 1094–1111, 2003.

Dubner R and Zeki SM. Response properties and receptive fields of cells in an anatomically defined region of the superior temporal sulcus in the monkey. *Brain Res* 35: 528–532, 1971.

Frazor RA, Albrecht DG, Geisler WS, and Crane AM. Visual cortex neurons of monkeys and cats: temporal dynamics of the spatial frequency response function. *J Neurophysiol* 91: 2607–2627, 2004.

Gautama T and Van Hulle MM. Function of center-surround antagonism for motion in visual area MT/V5: a modeling study. *Vision Res* 41: 3917–3930, 2001.

Hupe JM, James AC, Payne BR, Lomber SG, Girard P, and Bullier J. Cortical feedback improves discrimination between figure and background by V1, V2 and V3 neurons. *Nature* 394: 784–787, 1998.

Kapadia MK, Westheimer G, and Gilbert CD. Dynamics of spatial summation in primary visual cortex of alert monkeys. *Proc Natl Acad Sci USA* 96: 12073–12078, 1999.

Lagae L, Gulyas B, Raiguel S, and Orban GA. Laminar analysis of motion information processing in macaque V5. *Brain Res* 496: 361–367, 1989.

Lagae L, Raiguel S, and Orban GA. Speed and direction selectivity of macaque middle temporal neurons. *J Neurophysiol* 69: 19–39, 1993.

Levitt JB and Lund JS. Contrast dependence of contextual effects in primate visual cortex. *Nature* 387: 73–76, 1997.

Martinez-Trujillo J, and Treue S. Attentional modulation strength in cortical area MT depends on stimulus contrast. *Neuron* 35: 365–370, 2002.

Maunsell JH and Van Essen DC. Functional properties of neurons in middle temporal visual area of the macaque monkey. I. Selectivity for stimulus direction, speed, and orientation. *J Neurophysiol* 49: 1127–1147, 1983.

Mikami A, Newsome WT, and Wurtz RH. Motion selectivity in macaque visual cortex. I. Mechanisms of direction and speed selectivity in extrastriate area MT. *J Neurophysiol* 55: 1308–1327, 1986.

Moulden B, Kingdom F, and Gatley LF. The standard deviation of luminance as a metric for contrast in random-dot images. *Perception* 19: 79–101, 1990.

Polat U, Mizobe K, Pettet MW, Kasamatsu T, and Norcia AM. Collinear stimuli regulate visual responses depending on cell's contrast threshold. *Nature* 391: 580–584, 1998.

Priebe NJ, Cassanello CR, and Lisberger SG. The neural representation of speed in macaque area MT/V5. *J Neurosci* 23: 5650–5661, 2003.

Priebe NJ and Lisberger SG. Estimating target speed from the population response in visual area MT. *J Neurosci* 24: 1907–1916, 2004.

Prince SJ, Pointon AD, Cumming BG, and Parker AJ. Quantitative analysis of the responses of V1 neurons to horizontal disparity in dynamic random-dot stereograms. *J Neurophysiol* 87: 191–208, 2002.

Robinson D. A method of measuring eye movement using a scleral search coil in a magnetic field. *IEEE Trans Biomed Engin* 10: 137–145, 1963.

Rodman HR and Albright TD. Coding of visual stimulus velocity in area MT of the macaque. *Vision Res* 27: 2035–2048, 1987.

Sceniak MP, Ringach DL, Hawken MJ, and Shapley R. Contrast's effect on spatial summation by macaque V1 neurons. *Nat Neurosci* 2: 733–739, 1999.

Sclar G. Expression of "retinal" contrast gain control by neurons of the cat's lateral geniculate nucleus. *Exp Brain Res* 66: 589–596, 1987.

Shannon CE. A mathematical theory of communication. *Bell Syst Tech J* 27: 379–423, 1948.

Shapley RM and Victor JD. The effect of contrast on the transfer properties of cat retinal ganglion cells. *J Physiol* 285: 275–298, 1978.

Solomon SG, White AJ, and Martin PR. Extraclassical receptive field properties of parvocellular, magnocellular, and koniocellular cells in the primate lateral geniculate nucleus. *J Neurosci* 22: 338–349, 2002.

Stone LS and Thompson P. Human speed perception is contrast dependent. *Vision Res* 32: 1535–1549, 1992.

Tadin D, Lappin JS, Gilroy LA, and Blake R. Perceptual consequences of centre-surround antagonism in visual motion processing. *Nature* 424: 312–315, 2003.

van Hateren JH. Theoretical predictions of spatiotemporal receptive fields of fly LMCs, and experimental validation. *J Comp Physiol [A]* 171: 157–170, 1992a.

van Hateren JH. A theory of maximizing sensory information. *Biol Cybern* 68: 23–29, 1992b.

Weiss Y, Simoncelli EP, and Adelson EH. Motion illusions as optimal percepts. *Nat Neurosci* 5: 598–604, 2002.

Xiao DK, Raiguel S, Marcar V, Koenderink J, and Orban GA. Spatial heterogeneity of inhibitory surrounds in the middle temporal visual area. *Proc Natl Acad Sci USA* 92: 11303–11306, 1995.